Chapter 5

Heat Budget Analysis

The simulations achieved (chapter 4) allow us to compute the contribution of processes (atmospheric fluxes, horizontal advection, vertical advection, and vertical diffusion) to the heat budget of the upper central Arabian Sea. The simulations S2c (based on Fischer-based advective heat fluxes) and S3c (based on Reynolds-based advective heat fluxes) were selected for the analysis. Comparison between the two budgets allows a discussion of their robustness.

5.1 Fischer-based budget (S2c)

The contributions of the different processes to the total trend over the near-surface layer (0–50 m) and over the 0–250 m layer throughout the year are presented in Fig. 5.1 (a & b). In the near-surface layer, all processes (horizontal advection, vertical advection, vertical diffusion, and local air-sea fluxes) are important. In contrast, when the entire (0–250 m) layer is considered, the instantaneous balance is essentially between horizontal and vertical advection. Surface forcing plays a smaller role and vertical diffusion makes the smallest contribution. The trends of horizontal and vertical advective heat fluxes vary significantly at the scale of a few days to a few weeks. During most of the year, these two processes compete with each other to produce the resultant trend. The net contributions of the four processes to the heat content variations of the 0–50 m layer and of the 0–250 m layer were averaged (and integrated) over the 4 characteristic periods and for the whole year. The results are presented in Table 5.1 and Table 5.2.

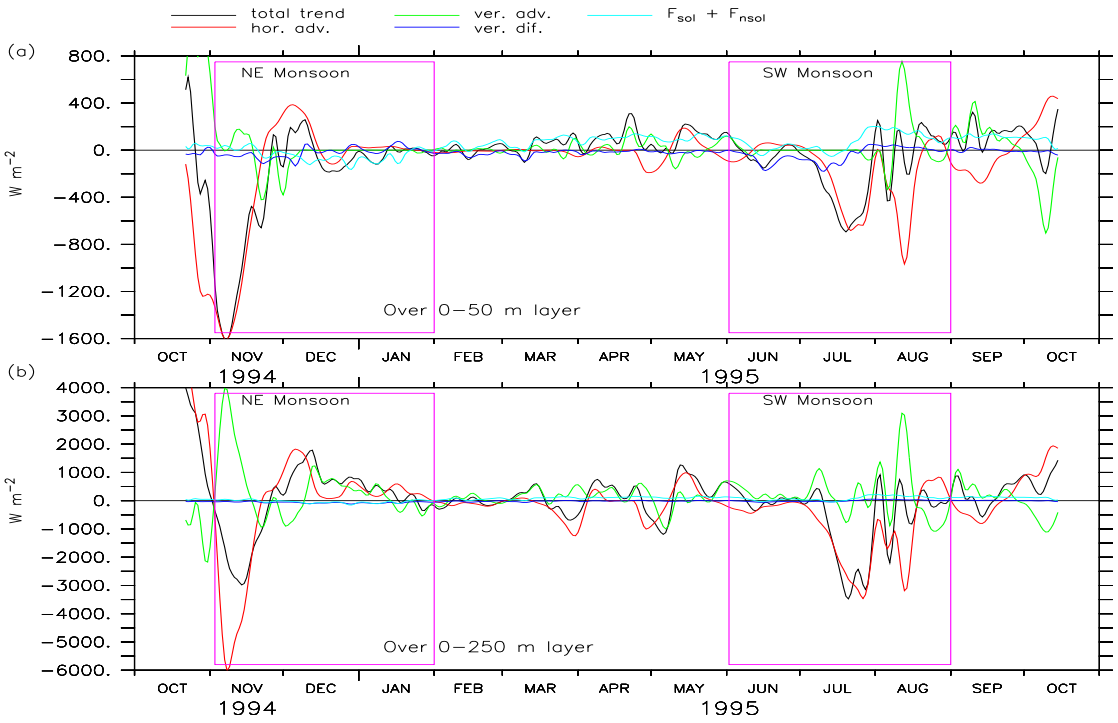

Figure 5.1: The contribution of different processes to the total temperature trend of the near-surface (0–50 m) layer (in units of heat fluxes) for simulation S2c: horizontal advection (red line); vertical advection (green line); vertical diffusion (blue line); combined non solar and solar local surface (heat) fluxes (cyan line). (b) same as (a), but for the 0–250 m layer. The monsoonal periods (NE Monsoon and SW Monsoon) in the figures are highlighted with pink rectangles. Note: the variables in the figure are smoothed by 7-day running mean.

5.1.1 Budget analysis for the 0–50 m layer

During the NE monsoon, the near-surface layer undergoes a net cooling of 1.68×10^9 J m^{-2} at the rate of (-220 W m^{-2}) (Table 5.1). This cooling results from the excess of heat loss through horizontal advection at the rate of 196 W m^{-2}, air-sea fluxes at the rate of 42 W m^{-2}, and vertical advection at the rate of 18 W m^{-2} over heating effects from vertical diffusion at the rate of 36 W m^{-2}. As shown in Fig. 5.1a, these four contributions vary significantly during this period. During early NE monsoon (November to mid-December), horizontal advection goes a large variation and provides large variability in the total trend. During rest of the NE monsoon, the total trend essentially results from comparable contributions from local surface fluxes, horizontal advection, and vertical diffusion.

Over the Spring IM, the near-surface layer gains 8.24×10^8 J m^{-2} heat at the rate of 79 W m^{-2}. This positive heating rate results mainly from the dominating heating effects of local air-sea fluxes (78 W m^{-2}) and from negligible contributions of other processes. As seen in Fig. 5.1a, most of the variability of the near-surface layer is dominated by local air-sea fluxes, whereas the remaining processes compensate each other.

The SW monsoon net cooling (8.53×10^8 J m^{-2}) of the near surface layer is achieved at the rate of 107 W m^{-2}. This cooling results from dominating cooling effects of horizontal advection at the rate of 183 W m^{-2} and from relatively smaller contribution of vertical diffusion at the rate of 26 W m^{-2} over opposing surface heating at the rate of 73 W m^{-2} and heating due to vertical advection at the rate of 29 W m^{-2}. The variability is at its highest for the four processes during this period (Fig 5.1).

The Autumn IM net warming (4.47×10^8 J m^{-2}) results at the rate of 110 W m^{-2}, with positive contributions from surface fluxes at the rate of 98 W m^{-2} and from horizontal advection at the rate of 25 W m^{-2}. Contributions of vertical advection and vertical diffusion are very small. During this period (similar to the Spring IM), the local air-sea fluxes mostly control the variability, with the remaining processes compensating each other (Fig. 5.1a).

The net cooling over the studied year (1.21×10^9 J m^{-2}) is achieved at the rate of 39 W m^{-2}. This cooling results from the excess heat removed by horizontal advection at the rate of 119 W m^{-2} over the positive heat input by surface forcing at the rate of 48 W m^{-2} and by vertical advection at the rate of 32 W m^{-2}. Contribution of vertical diffusion is negligible.

Table 5.1: Average and integrated heat content variation of the 0–50 m layer for simulation S2c (in W m^2 and J m^{-2}) during four characteristic periods of the year during 20 October 1994 to 17 October 1995 are presented. Negative values indicates heat loss from the ocean.

Rate of heat content variation Period	Resultant W m^{-2} (J m^{-2})	Local surface fluxes W m^{-2} (J m^{-2})	Horizontal advection W m^{-2} (J m^{-2})	Vertical advection W m^{-2} (J m^{-2})	Vertical diffusion W m^{-2} (J m^{-2})
NE Monsoon 1-Nov.-94 :31-Jan.-95	-220.2 (-1.68×10^9)	-41.62 (-3.31×10^8)	-196.4 $-1.56 \times 10^9)$	-18.38 (-3.42×10^8)	$+36.22$ $(+3.56 \times 10^8)$
Spring IM 1-Feb.-95:31-May-95	$+78.79$ $(+8.24 \times 10^8)$	$+77.72$ $(+8.19 \times 10^8)$	-7.49 (-7.83×10^7)	$+12.32$ $(+1.29 \times 10^8)$	-4.40 (-4.60×10^7)
SW Monsoon 1-Jun-95:31-Aug.-95	-107.40 (-8.53×10^8)	$+73.19$ $(+5.82 \times 10^8)$	-183.40 (-1.46×10^9)	$+29.35$ $(+2.33 \times 10^8)$	-26.52 (-2.10×10^8)
Autumn IM 1-Sep.-95:16-Oct-95	$+110.10$ $(+4.47 \times 10^8)$	$+100.5$ $(+4.00 \times 10^8)$	$+25.44$ $(+1.033 \times 10^8)$	-6.89 (-2.78×10^7)	-7.02 (-2.85×10^7)
Whole Year 20-Oct-94:16-Oct-95	-38.68 (-1.210×10^9)	$+48.3$ (1.52×10^9)	-119.2 (-3.74×10^9)	$+32.42$ $(+1.02 \times 10^8)$	-0.22 (-0.043×10^8)

Table 5.2: Average and integrated heat content variation of the 0–250 m layer for simulation S2c (in W m^{-2} and J m^{-2}) during four characteristic periods of the year during 20 October 1994 to 17 October 1995 are presented.

Rate of heat content variation Period	Resultant W m^{-2} (J m^{-2})	Local surface fluxes W m^{-2} (J m^{-2})	Horizontal advection W m^{-2} (J m^{-2})	Vertical advection W m^{-2} (J m^{-2})	Vertical diffusion W m^{-2} (J m^{-2})
NE Monsoon 1-Nov.-94 :31-Jan.-95	-5.30 (-4.21×10^7)	-41.62 (-3.31×10^8)	-334.5 (-2.66×10^9)	$+370.9$ $(+2.95 \times 10^9)$	-0.04 (-0.003×10^8)
Spring IM 1-Feb.-95:31-May-95	$+127.7$ $(+1.33 \times 10^9)$	$+100.0$ $(+1.05 \times 10^9)$	-93.3 (-9.75×10^8)	$+120.7$ $(+1.26 \times 10^9)$	$+0.07$ $(+0.006 \times 10^8)$
SW Monsoon 1-Jun-95:31-Aug.-95	-400.7 (-3.18×10^9)	$+89.9$ $(+7.15 \times 10^8)$	-720.7 (-5.73×10^9)	$+230.1$ $(+1.83 \times 10^9)$	-0.01 (-0.0006×10^8)
Autumn IM 1-Sep.-95:16-Oct-95	$+402.1$ $(+1.60 \times 10^9)$	$+119.0$ $(+4.72 \times 10^8)$	$+273.50$ $(+1.08 \times 10^9)$	$+5.69$ $(+3.85 \times 10^7)$	$+0.04$ $(+0.002 \times 10^8)$
Whole Year 20-Oct-94:16-Oct-95	$+44.61$ $(+1.40 \times 10^9)$	$+67.49$ $(+2.11 \times 10^9)$	-81.62 (-2.56×10^9)	$+162.6$ $(+5.085 \times 10^9)$	$+0.02$ (-0.006×10^8)

5.1.2 Budget analysis for the 0–250 m layer

As regards the whole simulated layer (Table 5.2), the NE monsoon net cooling (4.21×10^7 J m^{-2}) occurs at the rate of 5 W m^{-2}. This small rate of cooling is due to dominating effect of large heat losses through horizontal advection (335 W m^{-2}) and through the atmospheric fluxes (22 W m^{-2}) over large heating by vertical advection (370 W m^{-2}). As shown in Fig. 5.1, the competition between the horizontal and vertical advection during this period is significant. During early November to mid-December, vertical advection essentially opposes the large change in the trend caused by horizontal advection. During the rest of the NE monsoon, the total trend is mostly controlled by vertical advection; at this time, contribution of horizontal advection is much weaker.

The spring IM net warming (1.33×10^9 J m^{-2}) is achieved at the rate of 127 W m^{-2}. This warming rate is largely due to heating through the interface (100 W m^{-2}) and mutual competition between the heating due to vertical advection (120 W m^{-2}) and cooling due to horizontal advection

(93 W m^{-2}). Figure 5.1b shows that competition between the horizontal and vertical advection is mostly responsible for the variability in the total trend during this period.

The SW monsoon net cooling (3.18×10^9 J m^{-2}) is achieved at the rate of 400 W m^{-2}. This cooling results mainly from high heat removal by horizontal advection at the rate of 721 W m^{-2}, which is partially compensated by significant heating by vertical advection at the rate of 230 W m^{-2}; at this time, there is a relatively small positive influx through the interface (90 W m^{-2}). During this period, horizontal and vertical advection undergo high and similar variations (Fig. 5.1b).

The Autumn IM net warming (1.60×10^9 J m^{-2}) is achieved at the rate of 402 W m^{-2}. This warming results mainly from heating by horizontal advection at the average rate of 273 W m^{-2} and surface forcing at the average rate of 119 W m^{-2}. As seen in Fig. 5.1b, the large variability of the heating/cooling in total trends in heating is again largely due to the competition between horizontal and vertical advection.

The net warming over the studied year (1.40×10^9J m^{-2}) occurs at the rate of 45 W m^{-2}. This warming rate can be linked to heating by surface forcing (67 W m^{-2}) and vertical advection (163 W m^{-2}), which add up to offset the heat removed by horizontal advection (82 W m^{-2}). Contribution of vertical diffusion over the 0–250 m layer is small compared with the other terms: its value is two order of magnitude less than that of the other process. This process redistributes heat and its integrated contribution corresponds to small losses through the bottom.

In summary, horizontal advection is responsible for net cooling of the simulated surface layer, whereas vertical advection and surface forcing fluxes are both responsible for net warming. Local forcing is always important, but is dominant only during the Spring inter-monsoon. The SW monsoon is the period of highest heat content variation, and most of the heat gained through the air-sea interface over the year is evacuated at that time.

5.2 Reynolds-based budget (S3c)

The contributions of different processes to total (integrated) trend over the ML and over the whole simulated (0–250 m) layer throughout the year are presented in Fig. 5.2(a&b). In the ML, the important processes are horizontal advection, vertical diffusion, and local surface fluxes. Vertical advection plays a minor role. In contrast, when the entire 0–250 m layer is considered, vertical advection is important and often more important than horizontal advection; surface forcing plays a smaller role and contribution of vertical diffusion is smallest. It is also worth noting that all terms

vary with significant amplitudes at the scale of a few days to a few weeks. The net contribution of the four processes to the heat budget variations of the 0–250 m layer and of the 0–50 m layer were integrated over the four characteristic periods and for the whole year. The results are presented in Table 5.3 and Table 5.4.

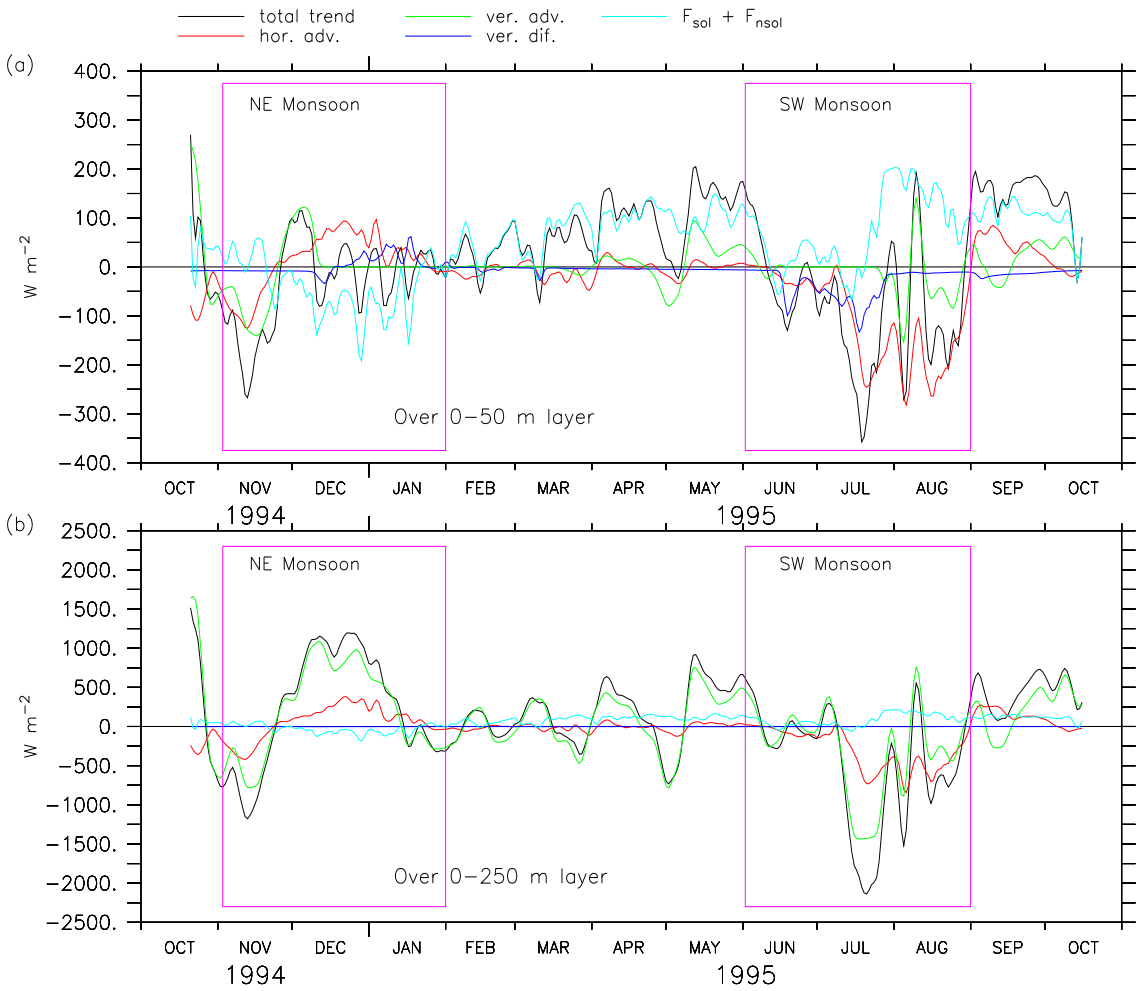

Figure 5.2: (a) The contribution of different processes to the total temperature trend for the 0–50 m layer (in units of heat flux) of the S3 simulation: horizontal advection (red line); vertical advection (green line); vertical diffusion (blue line); combined local surface fluxes and fluxes due to penetrating solar radiation (cyan line) in . (b) same as (a), but for the 0–250 m layer.

5.2.1 Budget analysis for the 0–50 m layer

During the NE monsoon, the near-surface layer undergoes a net cooling of 3.28×10^8 J m^{-2} at the rate of 41 W m^{-2} (Table 5.3). This cooling results from the excess of heat loss through air-sea fluxes at the rate of 42 W m^{-2} and vertical advection at the rate of 13 W m^{-2} over the heating effect of horizontal advection at the rate of 11 W m^{-2} and of vertical diffusion at the rate of 3 W m^{-2}. As shown in Fig. 5.2a, these four contributions vary significantly during this period. Vertical advection contributes significantly to the total trend only during early NE monsoon (mid-November to mid-December). During the rest of the NE monsoon, the total trend essentially results from comparable contributions from local surface fluxes, horizontal advection, and vertical diffusion.

Over the Spring IM, the near-surface layer gains 7.45×10^8 J m^{-2} at the rate of 71 W m^{-2}. This positive heating rate results mainly from the dominating heating effects of local air-sea fluxes (78 W m^{-2}) and from relatively very small contributions of other processes. As seen in Fig. 5.2a, most of the variability of the near-surface layer is dominated by local air-sea fluxes, whereas the remaining processes compensate each other.

The SW monsoon net cooling (7.1×10^8 J m^{-2}) of the near surface layer is achieved at the rate of 89 W m^{-2}. This cooling results from dominating cooling effects of horizontal advection at the rate of 107 W m^{-2}, and from the relatively smaller contribution of vertical diffusion at the rate of 34 W m^{-2}, and of vertical advection at the rate of 22 W m^{-2} over opposing surface heating at the rate of 73 W m^{-2}. The variability is at its highest for the four processes during this period (Fig 5.2a).

The Autumn IM net warming (2.72×10^8 J m^{-2}) results at the rate of 68 W m^{-2}, with positive contributions from surface fluxes at the rate of 101 W m^{-2} and from horizontal advection at the rate of 32 W m^{-2}; these processes which dominated over cooling effects from vertical advection at the rate of 51 W m^{-2}and vertical diffusion at the rate of 13 W m^{-2}. During this period (similar to the Spring IM), local air-sea fluxes mostly control the variability (Fig. 5.2a).

The net warming over the studied year (1.27×10^8 J m^{-2}) is achieved at the rate of 15 W m^{-2}. This warming results from the positive input by surface forcing at the rate of 48 W m^{-2}, which offsets the heat removed by horizontal advection at the rate of 24 W m^{-2}, by vertical diffusion at the rate of 11 W m^{-2}, and by vertical advection at the rate of 9 W m^{-2}.

Table 5.3: Average and integrated heat content variation of the 0–50 m layer for simulation S3c (in W m^{-2} and J m^{-2}) during four characteristic periods of the year during 20 October 1994 to 17 October 1995 are presented.

Rate of heat content variation Period	Resultant W m^{-2} (J m^{-2})	Local surface fluxes W m^{-2} (J m^{-2})	Horizontal advection W m^{-2} (J m^{-2})	Vertical advection W m^{-2} (J m^{-2})	Vertical diffusion W m^{-2} (J m^{-2})
NE Monsoon 1-Nov.-94 :31-Jan.-95	-41.26 (-3.28×10^8)	-41.62 (-3.31×10^8)	$+10.82$ $(+0.86 \times 10^8)$	-13.20 (-1.05×10^8)	$+2.73$ (0.22×10^8)
Spring IM 1-Feb.-95:31-May-95	$+70.73$ $(+7.45 \times 10^8)$	$+77.72$ $(+8.19 \times 10^8)$	-5.69 (-0.63×10^8)	$+3.16$ $(+0.33 \times 10^8)$	-4.14 (-0.44×10^8)
SW Monsoon 1-Jun-95:31-Aug.-95	-89.00 (-7.1×10^8)	$+73.19$ $(+5.82 \times 10^8)$	-106.6 (-8.47×10^8)	-21.55 (-1.71×10^8)	-34.06 (-2.71×10^8)
Autumn IM 1-Sep.-95:16-Oct-95	$+68.5$ $(+2.72 \times 10^8)$	$+100.6$ $(+4.00 \times 10^8)$	$+31.6$ $(+1.26 \times 10^8)$	-50.77 (-2.02×10^8)	-12.99 (-0.52×10^8)
Whole Year 20-Oct-94:16-Oct-95	$+4.04$ $(+1.268 \times 10^8)$	$+48.31$ $(+1.52 \times 10^9)$	-24.36 (-7.64×10^8)	-8.66 (-2.72×10^8)	-11.24 (-3.53×10^8)

Table 5.4: Average and integrated heat content variation of the 0–250 m layer for simulation S3c (in W m^{-2} and J m^{-2}) during four characteristic periods of the year during 20 October 1994 to 17 October 1995 are presented.

Rate of heat content variation Period	Resultant W m^{-2} (J m^{-2})	Local surface fluxes W m^{-2} (J m^{-2})	Horizontal advection W m^{-2} (J m^{-2})	Vertical advection W m^{-2} (J m^{-2})	Vertical diffusion W m^{-2} (J m^{-2})
NE Monsoon	$+127.7$	-41.62	$+55.9$	$+114.8$	-1.3
1-Nov.-94 :31-Jan.-95	$(+1.01 \times 10^9)$	(-3.31×10^8)	$(+4.44 \times 10^8)$	$(+9.12 \times 10^8)$	(-1.06×10^7)
Spring IM	$+124.9$	$+100.0$	-9.07	$+36.35$	-1.75
1-Feb.-95:31-May-95	$(+1.32 \times 10^9)$	$(+1.05 \times 10^9)$	(-9.56×10^7)	$(+3.83 \times 10^8)$	(-1.84×10^7)
SW Monsoon	-388.4	$+89.9$	-292.1	-185.1	-1.2
1-Jun-95:31-Aug.-95	(-3.09×10^9)	$(+7.15 \times 10^8)$	(-2.32×10^9)	(-1.47×10^9)	(-0.9×10^7)
Autumn IM	$+311.5$	$+119.0$	$+108.9$	$+84.39$	-0.72
1-Sep.-95:16-Oct-95	$(+1.24 \times 10^9)$	$(+4.72 \times 10^8)$	$(+4.33 \times 10^8)$	$(+3.35 \times 10^8)$	(-0.2×10^7)
Whole Year	$+57.3$	$+67.31$	-56.1	$+47.35$	-1.36
20-Oct-94:16-Oct-95	$(+1.80 \times 10^9)$	$(+2.11 \times 10^9)$	(-1.76×10^9)	$(+1.48 \times 10^9)$	(-4.27×10^7)

5.2.2 Budget analysis for 0–250 m layer

As regards the whole simulated layer (Table 5.4), the NE monsoon net warming (1.01×10^9 J m^{-2}) occurs at the rate of 128 W m^{-2}. This rate of warming is largely due to vertical advection (115 W m^{-2}) and to horizontal advection (56 W m^{-2}), with relatively small losses through the air-sea interface (42 W m^{-2}). As shown in Fig. 5.2b, the variation of horizontal and vertical advection during this period is significant.

The spring IM net warming (1.32×10^9 J m^{-2}) is achieved at the rate of 125 W m^{-2}. This warming rate is largely due to heating through the surface (100 W m^{-2}) and to vertical advection (37 W m^{-2}), with negligible cooling effects from horizontal advection and vertical diffusion. Figure 5.2b shows that vertical advection is mostly responsible for the variability in the total trend during this period.

The SW monsoon net cooling (3.1×10^9 J m^{-2}) is achieved at the rate of (388 W m^{-2}). This cooling results mainly from high heat removal by horizontal advection at the rate of (292 W m^{-2}) and by vertical advection at the rate of (185 W m^{-2}). At this time, there is a relatively small positive influx through the surface (90 W m^{-2}). During this period, horizontal and vertical advection undergo high and similar variations (Fig. 5.2b).

The Autumn IM net warming (1.24×10^9 J m^{-2}) is achieved at the rate of 311 W m^{-2}. This warming results mainly from heating by surface forcing at the average rate of 119 W m^{-2}, horizontal advection at the average rate of 108 W m^{-2}, and vertical advection at the average rate of 84 W m^{-2}. As seen in Fig. 5.2b, the large variability of the heating/cooling in total trends in heating is again largely due to vertical advection.

The net warming over the studied year (2.92×10^9J m^{-2}) occurs at the rate of 93 W m^{-2}. This warming rate can be linked to heating by vertical advection (162 W m^{-2}), and surface forcing (67 W m^{-2}), which add up to offset the heat removed by horizontal advection (136 W m^{-2}). Contribution of vertical diffusion over the 0–250 m layer is small compared with the other terms: its value is one order of magnitude less than that of the other process. This process redistributes heat and its integrated contribution corresponds to small losses through the bottom.

In summary, horizontal advection is responsible for net cooling of the simulated surface layer, whereas vertical advection and surface forcing fluxes are both responsible for net warming. Local forcing is always important, but is dominant only during the Spring inter-monsoon. The SW monsoon is the period of highest heat content variation, and most of the heat gained through the air-sea interface over the year is evacuated at that time.

5.3 Comparison between Fischer-based and Reynolds-based budgets

Figures 5.3 and 5.4 present the heat budget based on S2c and S3c together with 2 other concurrent simulations: S2c* and S3b. S2c* was carried out in place of S2c simulation to improve on the S2c simulation in section 4.2.1.1 by assigning zero fluxes to the Fischer-based horizontal advective heat fluxes within the ML during the early NE monsoon (20 October to mid–November). S3b is similar to S3c, excepted that the SODA vertical velocity was used instead of the predicted (from Reynolds-based horizontal advective heat fluxes) vertical velocity.

5.3.1 0–50 m layer

The predicted net cooling over 0–50 m layer in S2c is 3 times larger than the cooling present in observations, whereas the predicted cooling in S3c is 20% smaller than the observations. In S2c simulation, horizontal advection drives a large cooling and vertical diffusion drives a large heating in the surface layer. In contrast, horizontal advection drives heating and vertical diffusion drives negligible heating in the S3c surface layer budget. The contribution of horizontal advection is relatively small in S2c* simulation as compared with S2c simulation, and contribution due to vertical diffusion in S2c* is almost the same as in S2c. The contributions of various processes in S3b and S3c are similar.

During the SW monsoon, the dominating role of horizontal advection in cooling the surface layer over the heating effects from the atmospheric fluxes is shown by all the simulations.

The dominating role of atmospheric fluxes in heating the surface layer is depicted from all the four simulations during the Spring and Autumn IM. The total heat content variation in both S2c and S3c during the SW monsoon and during the IMs are almost the same as in the observations.

Regarding the whole year, S3c and S3b suggest that the net heating of the surface layer is dominated by atmospheric fluxes over cooling caused by horizontal advection and vertical diffusion with small contribution from vertical advection. The predicted heating in S3c is almost equal to the heating present in the observations. In contrast, the S2c simulation suggests that the near-surface layer undergoes large cooling (instead of the warming present in observation) owing to excess cooling due to horizontal advection, which dominates the comparable warming caused by vertical advection and atmospheric fluxes. The large biasing during the NE monsoon in S2c simulation affects the whole year.

5.3.2 0–250 m layer

In all four simulations S2c, S2c*, S3c, and S3b, the total budget for (0–250 m) layer during the NE monsoon is positive (warming) mainly due to the dominating effect of vertical advection; however, the amplitude of variation of vertical advection differs in different simulations due to the different contributions from horizontal advection (see Fig. 5.4). In S2c (S2c*) simulation vertical advection causes large warming, which dominates the large cooling caused by horizontal advection. In contrast, vertical advection and horizontal advection both cause warming in S3c (S3b) simulation, and their amplitudes are relatively much smaller than the corresponding contributions in S2c.

During the Spring IM, all the four simulations suggest that atmospheric fluxes and vertical advection together play a role in heating the 0–250 m layer. In S3c (S3b), the contribution of vertical

advection is relatively smaller than atmospheric fluxes. The contribution of vertical advection is larger than atmospheric fluxes in S2c (S2c*).

The SW monsoon cooling of the layer comes from both horizontal and vertical advection in S2c simulation. In contrast, the cooling effect of horizontal advection dominates the heating effect of vertical advection in S3c simulation.

During the Autumn IM, all the four simulations suggest that atmospheric fluxes and horizontal advection together play a role in heating the layer. The role of vertical advection is negligible in S2c, in contrast to the comparable horizontal advection contribution of vertical advection in S3c.

Regarding the whole year, both simulations suggest that the net heating of the layer comes from comparable contributions from horizontal advection, vertical advection, and atmospheric fluxes. In S2c, contributions of vertical advection and horizontal advection are larger than the corresponding contributions in S3c simulation.

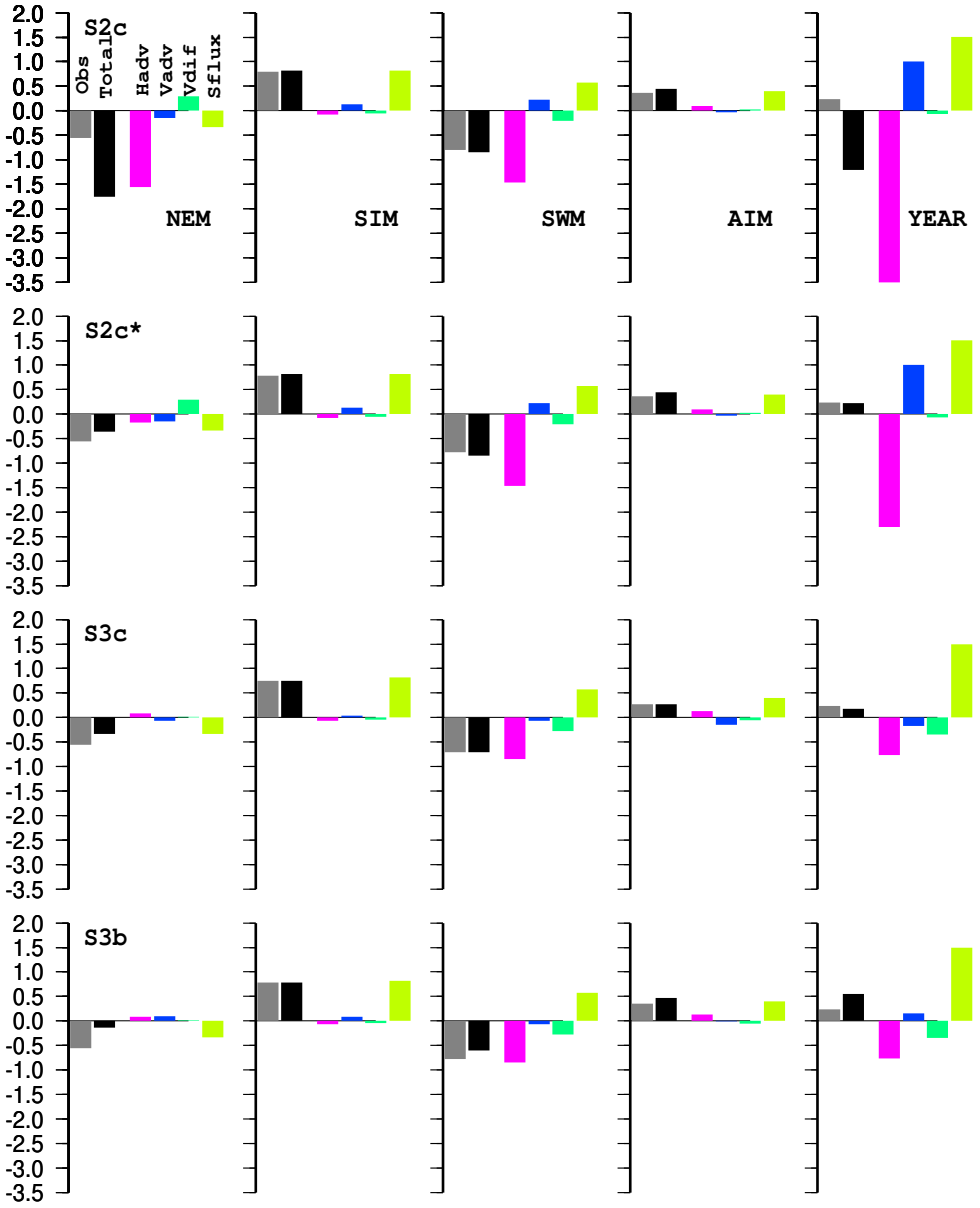

Figure 5.3: Barplots showing the contribution of various heat budget terms for the near–surface (0–50 m) layer: horizontal advection (magenta), vertical advection (blue), vertical diffusion (cyan), and surface heat flux (green) in the net heat content (black).The total predicted (black) and observed (grey) heat content variations of different monsoon periods also presented. Along the vertical the values are: $X \times 10^9$J m^{-2}. The upper panel: S2c simulation, 2nd panel: S2c* simulation, 3rd panel: S3c simulation, and lower panel: S3b simulation.

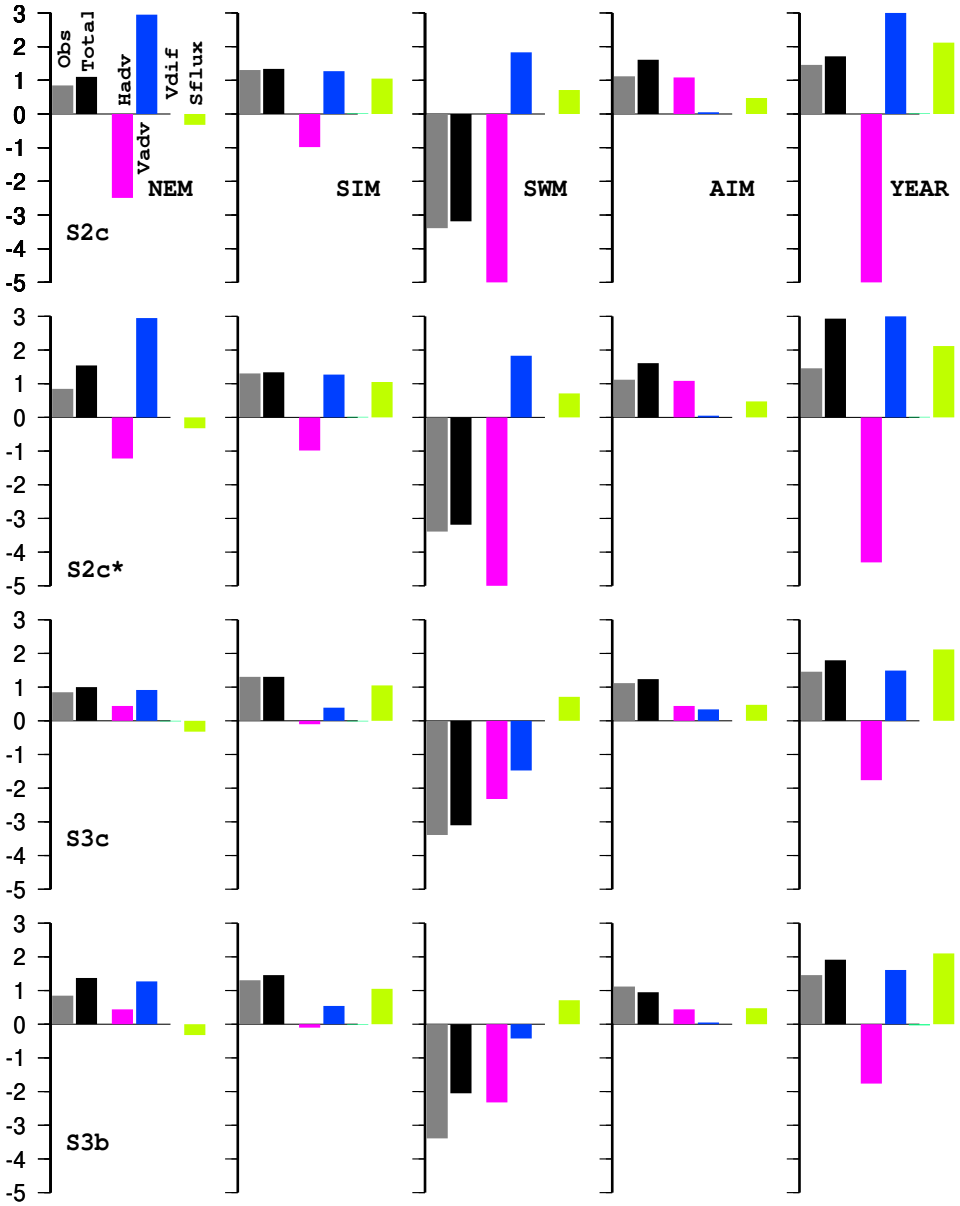

Figure 5.4: Barplots showing the contribution of various heat budget terms for the whole (0–250 m) layer: horizontal advection (magenta), vertical advection (blue), vertical diffusion (cyan), and surface heat flux (green) in the net heat content (black).The total predicted (black) and observed (grey) heat content variations of different monsoon periods also presented. Along the vertical the values are: $X \times 10^9$J m^{-2}. The upper panel: S2c simulation, 2nd panel: S2c* simulation, 3rd panel: S3c simulation, and lower panel: S3b simulation.

5.4 Concluding remarks

The contribution of vertical diffusion during the NE monsoon in S2c simulation is large and positive in 0–50m layer budget and almost equal to that of the atmospheric fluxes. This large and positive contribution of vertical diffusion seems to be suspicious. The analysis of the predicted profiles of diffusive heat fluxes suggest that the large values of the flux result from the strong cooling induced by Fischer-based horizontal advection within the mixed layer during November–December.

The results of heat budget analysis based on S3b (SODA-based) simulation are almost similar to the results of the analysis based on S3c simulations.

In most of the cases, the above heat budget analyses for S2c and S3c simulations lead to different inferences. This is because of the fact that the heat fluxes due to vertical advection used for the heat budget analysis are dependent on magnitudes of horizontal advective heat fluxes (as they were calculated as the residual terms of the model heat budget). Although it is difficult to arrive any independent conclusion about the relative contributions of horizontal and vertical advection, it can be believed that both the processes are important throughout the year.

For the near surface (0–50 m) layer, some important conclusions can be derived. During IMs, atmospheric fluxes are the dominating processes and during the NE and SW monsoons, all processes are important. The horizontal advection is the most dominating process during the SW monsoon.

The contributions of various heat budget terms in simulation S2c (S2c*) exhibited large amplitudes during both the monsoon periods and it is difficult to believe that they are realistic. As already described in section 4.2.4, the resultant predicted vertical velocity (and hence vertical advection) that is used in S2c simulation is largely sensitive to a 50% change in the Fischer-based horizontal advection during the SW and NE monsoons. In contrast, the predicted vertical velocity that is used in S3c simulation remains unchanged with respect to a 50 % change in Reynolds-based advective heat flux estimates. Hence, we infer that, owing to the uncertainty associated with Fischer-based estimates, the actual heat fluxes due to horizontal advection must be much weaker than in Fischer-based estimates. If this is so, the heat budget based on S3c simulation is the most representative of the location of the mooring array.